Evolution of Porosity–Permeability Relationships in Bio-Mediated Processes for Ground Improvement: A Pore-Scale Computational Study

Sina Nassiri, A.M.ASCE[1]; and Nariman Mahabadi, Ph.D., A.M.ASCE[2]

[1]Ph.D. Student, Dept. of Civil Engineering, Univ. of Akron, Akron, OH.
Email: sn173@uakron.edu
[2]Assistant Professor, Dept. of Civil Engineering, Univ. of Akron, Akron, OH.
Email: nmahabadi@uakron.edu

ABSTRACT

Bio-mediated techniques are among biogeochemical processes in subsurface that have been introduced as alternatives to conventional methods for soil improvement. These processes can alter hydraulic properties of the subsurface through a complex veriety of coupled processes including the interaction of biomineral–biogas–biofilm with the solid matrix and pore structure of the soil. A clear understanding of these obscure interactions is critical to study the impact of bio-geochemical processes on the hydrology and predict reactive transport phenomena within the treatment zones. In this study, a 3D pore network model is extracted by CT imaging from a sandy soil sample. Various scenarios resembling different biogeochemical products and contents are numerically assigned into the networks. Simulations including evolution of pore-scale characteristics and Representative Elementary Volume (REV) scale porosity–permeability relationships are investigated. The results show that the hydraulic properties of bio-treated soils are dramatically affected by the spatial distribution, heterogeneity, and pore-habit of the products of bio-mediated processes.

INTRODUCTION

Bio-geochemical processes can be introduced to remediate contaminated soils, modify the mechanical response of the sediments, and recover resources through various techniques such as air sparging or gas exsolution by supersaturated water injection for soil remediation (Enouy et al., 2011; McCray & Falta, 1997), Microbially Induced Carbon Precipitations (MICP) and Microbial Induced Desaturation and Precipitation (MIDP) for liquefaction mitigation (van Paassen, 2009; Whiffin et al., 2007; DeJong et al., 2009; Stallings Young et al., 2021), and microbial biofilm development for creating hydraulic barriers (Cunnningham et al. 2003). In this context, the products of bio-geochemical processes can be caterogrozied into the three groups of biogenic gases (gas phase), biominerals (solid phase) and biofilms (semi solid-liquid phase). However, alteration in the pore structure can occur through a complex veriety of coupled processes including the interaction of biogas-bomineral-biofilm with the soil matrix and fluids in the subsurface. A clear understanding of these complex interactions are critical to study the impact of bio-geochemical processes on the hydrology of subsurface and predict reactive transport phenomena in sediments. Although alteration in the soil occure at the pore-scale, the scales of the engineering problems are typically much larger. As a result, it is often more computationally efficient that the impacts of such changes to the saturated flow properties of soil be explained by generalized hydarulic properties, the permeability. By using these averaged concepts, modelers can avoid the need for a detailed characterization of the fluid-soil matrix

interface at the expense of losing information regarding hydrodynamics of fluid in pore-scales. To translate pore-scale alterations to REV-scales, hydarulic properties can be related to another averaging REV-scale paramter, the porosity (Hommel et al., 2018). However, an accurate, quantitative description of the changes of porosity and its impacts on flow dynamics is essential for transport modelling in bio-treated soils.

In this study, we aim to explore various bio-geochemical mechanisms that alter the hetergoeneity of pore-structure and investiage their impacts on the hydrodynamics of the porous media from pore-scale to REV-scale. The investigation was done on a 3D pore network model (PNM) which had been extracted by CT imaging from a sandy sediment. Several pore-clogging scenarios including pore-filling and load-bearing (throat-filling) with varying contents and clogging mechanisms are applied to the PNM. The evolution of porous media are explored by performing fluid flow simulations on the PNM. Pore-scale charactersitics of the bio-treated soil sample such as local changes in hydrodynamics, tortousity and percolation pathways, and REV-scale properties including the porosity-permeability relationships are investigated. The applicabiliy of theoretical/emperical relationships such az Kozeny-Carman and Power-law relations in bio-treated sediments are studied.

METHODOLOGY

Pore Network Model. In order to investigate the effect of biochemical clogging on the porous media and its hydrodynamic behavior, a significant series of Computational Fluid Dynamics (CFD) simulations are required. However, due to the complexity involved in natural porous systems, direct numerical methods such as Finite Element Methods which requires mesh generation on the entire domain geometry and solving partial differential equations are prohibitively time consuming and expensive. To overcome this limitation, the numerical simulations performed in this study are formed around several numerical algorithms developed by Mahabadi et al. 2016, and Mahabadi and van Passen (2020) which aims to study complex coupled bio-chemical processes in highly heterogenous porous media of soil and rock systems. The basis of these algorithms is built on the concept of Pore Network Models (PNM) proposed by Dong and Blunt (2009). A PNM consists of interconnected networks of nodes (Pores) and tubes (throats) as shown in Figure 1a which can be either directly extracted from natural sediments or numerically generated to simplify and satisfy the geometry of the original natural porous network. Using the PNM, one can efficiently simulate the flow of a viscous fluid in the entire network by considering the conservation of mass and solving Hagen-Poiseuille equation which can significantly reduce the computational cost of numerical simulations (Mahabadi and Jang 2014).

The investigated pore network in this study was extracted from X-ray scanning of a soil sample recovered from Mallik 5L-38 site in Beaufort Sea, Canada. The grain size distribution of the sediment is presented in Figure 1b. The total volume of scanned sediment was 27 mm^3 (3 mm×3 mm ×3 mm) with 12.5 μm/pixel resolution. The resulted CT images provide the 3D structure of the sediment (soil grains), and the pore space (voids) (Figure 1c, left and middle). Having this information, a three-dimensional pore network was extracted using maximall ball algorithm (Dong and Blunt 2009). This algorithm generates spheres inscribed in the pore space, where the bigger spheres turn into the pores of the PNM and the size of smaller spheres located in pore throats are used as the radii of cylindrical tubes connecting the neighboring pores. The result is the PNM consisting the interconnected network of spherical pores and cylindrical tubes

(Figure 1c, right). The extracted pore network in this study consists of 4591 pores connected via 18871 tubes, with the mean connectivity number of 6.8 per pore (coordination number *cn*=6.8). Mean pore radius is 69 µm and the mean tube radius is 12 µm. Figure 1d, indicates the radii and their distribution for spherical pores and cylindrical tubes, with their normalized frequency where actual numbers of pores and tubes are presented in the inset of Figure 1d.

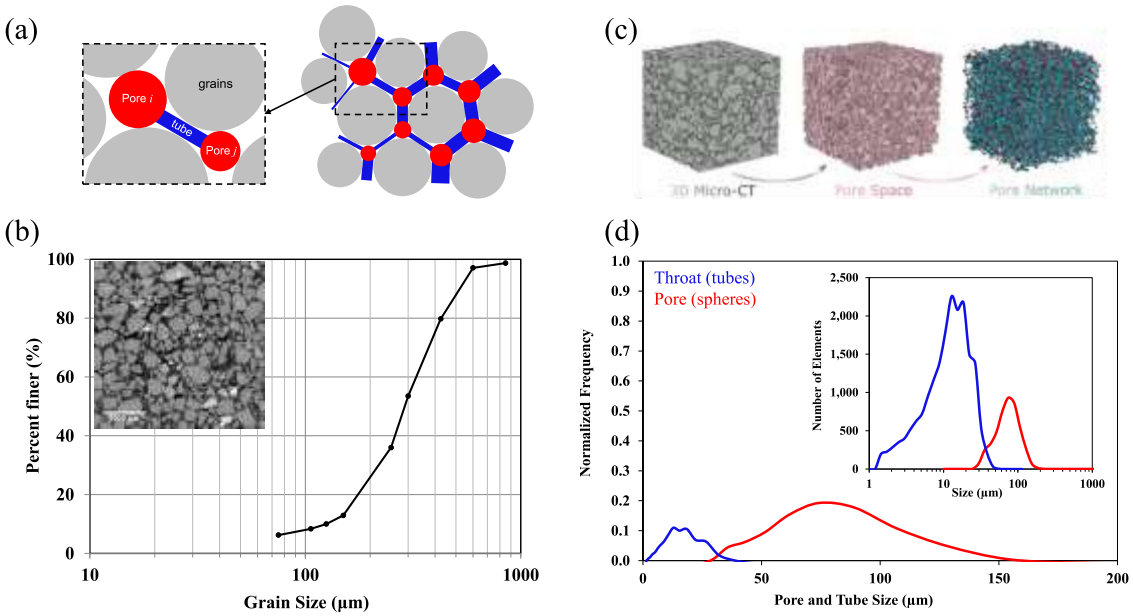

Figure 1. Pore network extraction and properties; a) Conceptual illustration of a pore network model in a soil packing; b) Grain size distribution of the X-ray scanned soil sample; c) Pore network extraction from the X-ray scanning of the soil sample; d) Pore and tube size distribution of the extracted PNM

Bio-clogging in PNM. Bioclogging clogging in subsurface is the process of pore space clogging via bio-geochemical reactions and their natural or synthesized products which can be categorized into the formation of biominerals, biogas bubbles and biofilms. These products may cement the surface or contact points of soil particles or fill the voids of the porous media which will eventually change the hydraulic behavior of the soil medium. In this study, we aim to explore three main clogging formation mechanisms. 1) Load bearing (Throat filling): this scenario results in the filling of throat regions where the clogging was simulated by the elimination of random tubes; 2) Distributed pore filling: clogging occurs in random voids in which simulations are performed by random selection and elimination of individual pores; 3) Local pore filling: clogging occurs in certain regions of the sediment within a group of pores (pore clusters). Local pore filling is simulated by selecting a random pore and filling its neighbor pores for a target clogging zone. The target clogging distance is changed to provide insights regarding the impact of cluster size on the simulation results. Three cluster size of 4-pores (small), 64-pores (medium), and 1024-pores (large) were investigated in this study.

In all the clogging scenarios, incremental clogging volumes were assigned from 0% (no clogging) to 100% (fully clogged). As the location of clogged pores impact the results, we explored the impact of clogging zone by considering three different randomized locations for each clogging scenario. Figure 2a shows the simulation cases for 15% clogging with distributed

pore filling and local pore filling (ranging from small to large cluster size). Figure 2b presents the clogged PNM for a local pore filling scenario with varying clogging contents, and Figure 2c shows the clogged PNM for a local pore filling scenario (with large cluster size) with varying spatial locations.

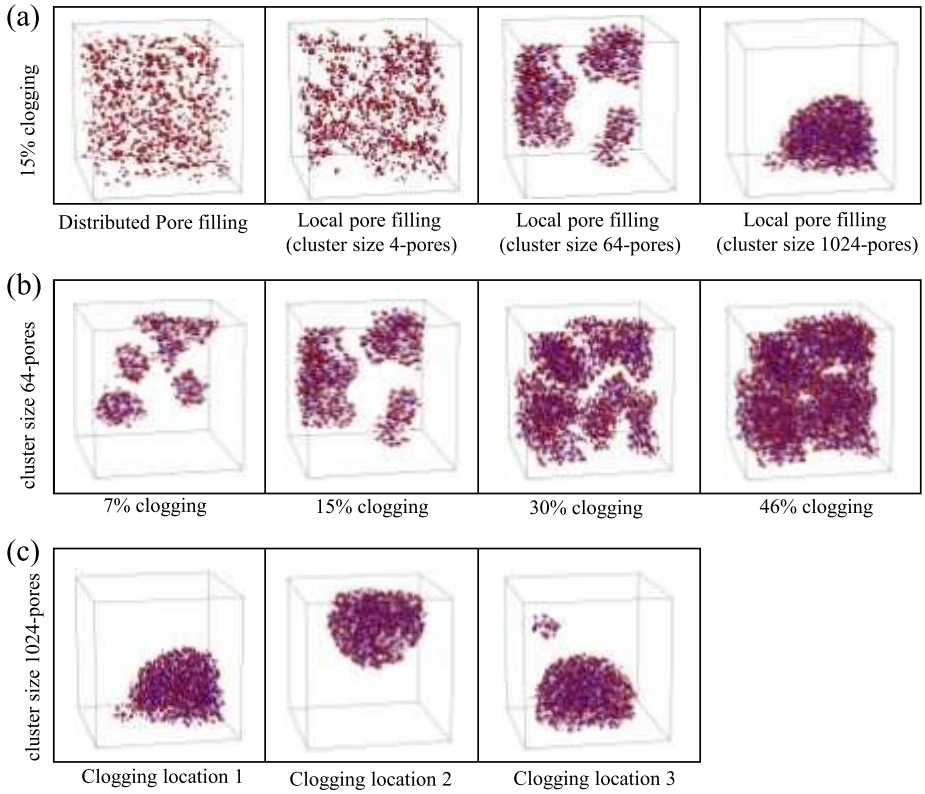

Figure 2. Clogged scenarios: a) 15% pore-filling in various cluster sizes; b) Various clogging percentages for cluster size 64-pores (medium); c) Different spatial locations of a large cluster (1024-pores) at a given clogging percentage of 15%.

Porosity-Permeability Simulation. We investigated the impact of bio-clogging on the porosity-permeability relationships in single-flow saturated conditions. Porosity of soil sample was computed by calculating the summation of total volume of non-clogged pores and tubes over the total volume of the soil sample. For permeability calculation, a differential pressure was assigned to the network at the pores connected to the inlet and outlet (left and right boundary). By the mass conservation law, the total flow rate into a pore (node) equals the total flow rate out of the node. The mass balance equation applied to all the internal nodes, resulting in a system of linear equations. By solving this system of linear equations, the internal pressure of all the pores in the network can be achieved. Now, consider two neighboring pores which are connected by a cylindrical tube. Using Hagen-Poiseuille equation, flow rate q through the tube is a function of fluid viscosity μ, tube radius R_{tube}, tube length L, and pressure difference between the neighboring pores ΔP:

$$q = \frac{\pi R_{tube}^4 \Delta P}{8\mu L} \tag{1}$$

Based on the differential pressure at the both end of each tube, as well as the tube radius and length, hydraulic gradient and flowrate in each tube was calculated via Darcy`s Law. The total flowrate of the sample was obtained by the summation of the flowrate of all the tubes connected to the outlet of the sample. The cross-section area of soil sample perpendicular to the flow path at the outlet was considered and coupled with the sample flowrate to obtain the soil sample permeability. The permeability at each stage of simulation for variety of clogging scenarios and contents (clogging percentages) were simulated.

RESULTS

Porosity-Permeability relationship. The clogging scenarios considered in this study are illustrated in Figure 3-right. In addition to the permeability computed by PNM numerical simulations, Kozeny-Carman (Le Gallo et al. 1998) analytical solution is used to estimate the permeability based on the porosity of clogged PNM. The general form of Kozeny-Carman equation can be written as:

$$K = \frac{n^3}{\tau(1-n)^2 S^2} \tag{2}$$

Where K is permeability, n is porosity, τ is the tortuosity, and S is the specific surface area of the grains. However, as the calculation of tortuosity and specific surface area is difficult in practice, it is more common to use only the porosity change to estimate the permeability reduction using the Kozeny-Carman equation. In order to generalize the effect of porosity change on permeability, the porosity and permeability can be normalized with respect to their initial conditions: initial porosity n_o and initial permeability K_o (prior to clogging). In this case, the estimation of permeability reduction can be achieved through the following equation:

$$\frac{K}{K_o} = \frac{n^3(1-n_o)^2}{n_o^3(1-n)^2} \tag{3}$$

Based on the Kozeny-Carman method, the porosity of the soil sample plays a crucial role in the permeability. In order to validate this notion and demonstrating the accuracy of this method, the estimated permeability via Kozeny-Carman method and simulated permeability should be compared. The normalized porosity-permeability (n′-K′) results are presented in Figure 3-left. The results indicate that the spatial distribution and pore habit of the clogging mechanisms play a significant role on the permeability of bio-clogged soils. At a given bio-product content (clogging percentage), the reduction in permeability varies dramatically depending on the pore-scale characteristics of the bio-clogging processes. For example, at a same clogging percentage (10%) indicating $n'=0.9$, $K'_{TF}=0.34$, $K'_{DPF}=0.62$, $K'_{LPF-small}=0.64$, and $K'_{LPF-large}=0.8$.

Simulations explain that the most sensitive scenario to permeability reduction is Throat-Filling (TF). In this case, the termination n', the normalized porosity at which the permeability is terminated (no flow condition), is about 0.8 (only 20% porosity reduction). The impact of porosity change is less in all the pore-filling scenarios compare to TF scenario. Since throats provide pore connections, elimination of a single throat would result in losing the connectivity of the entire neighboring pores. In this case, even a small clogging through TF mechanism may lead to a notable reduction in permeability compare to the pore filling mechanisms. The permeability of treated soils can also be affected by the spatial distribution of the bio-products at a given

clogging scenario. The data points presented in Figure 3 shows the three different randomized clogging spatial distribution for each scenario while the solid lines present the averaged lines. In the TF scenario, the data points have minimal deviations at a given porosity, indicating that permeability is not impacted by the spatial distribution of bio-products, but only affected by the amounts of bio-products. However, the spatial distribution plays an important role in the local pore filling mechanism (LPF), particularly when the size of clusters is large compare to the size of the soil sample (LPF-large cluster). Although at a given porosity, number of bio-products are equal for all the clogging scenarios, pore-filling with larger clusters allows the flow to be routed around the clogged area, however more distributed scenarios (e.g., Distributed-pore filling) tend to uniformly block the percolations pathways.

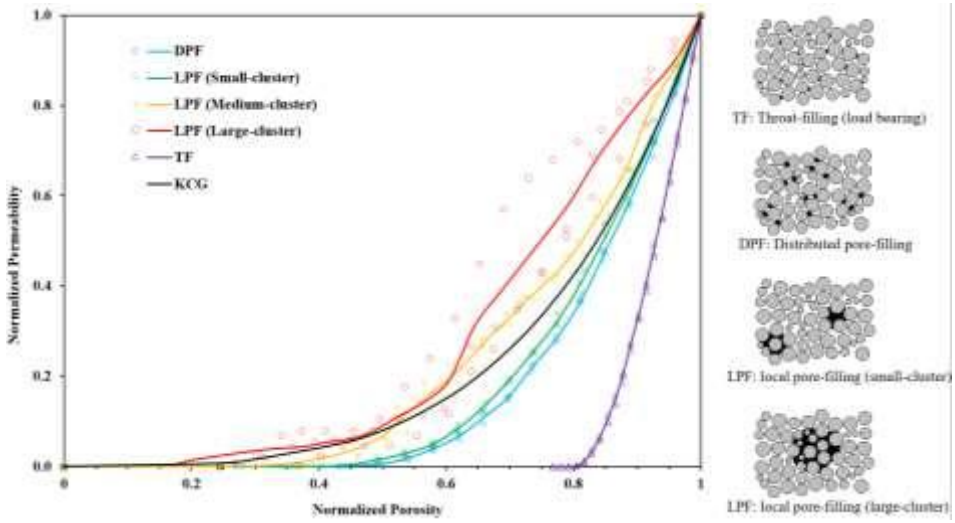

Figure 3. Schematic view of clogging in PNM for different clogging scenarios; porosity-permeability in various clogging scenarios.

Figure 3 also shows the inaccuracy of Kozeny-Carman to estimate permeability in different bio-clogging scenarios. Although Kozeny-Carman relatively estimates the permeability reduction for medium-size cluster clogging (LPF-medium size), it overestimates the DPF and LPF-small scenarios, and underestimates LPF-large scenario. As Eq. 3 solely relies on porosity and neglecting other pore-scale parameters, using Kozeny-Carman with considering only porosity result in an inaccurate estimation of permeability for various clogging mechanisms. The relation between changes in porosity and permeability relies on pore morphology since in pore-scales, the pore geometry determines the resistance to the fluid flow. However, in REV scale, fluid flow depends on the upscaled permeability parameters which integrate all the effects of sub-REV-scale geometries. Although changes in permeability are typically correlated with porosity, they can be affected by changes of other REV-scale parameters which are linked to the pore geometry, such as tortuosity and specific surface area (Ives and Pienvichitr 1965; Mostaghimi et al. 2012). Thus, in order to improve the computed permeability via Kozeny-Carman method, we investigated the effect of tortuosity, τ, and specific surface area, S. Considering the impact of tortuosity, and specific surface area, Eq. 3 can be rewritten as:

$$\frac{K}{K_o} = \frac{n^3(1-n_o)^2\tau_o S_0^2}{n_o^3(1-n)^2\tau S^2} \tag{4}$$

Consider a flow through a soil medium in which fluid carries via multiple flow paths (percolation paths). In a PNM, these percolation paths flow via a network of tubes that connects inlet to outlet pores. In this study, tortuosity is defined and calculated as the ratio of the average percolation length to the direct distance between the inlet and outlet ($\tau = \frac{L_{percolation}}{L_{sample}}$).

Figure 4 shows the percolation paths for different clogging scenarios and percentages. The results illustrate that tortuosity is affected by spatial distribution, content and mechanisms of bio-clogging. In general, increase in clogging results in tortuosity increase since the flow must bypass existing blockage to continue its path, which in turn increases the length of percolation path. However, at very large clogging contents, tortuosity can decrease occasionally. This is a special event in which highly clogged porous media results in fewer and shorter percolation paths. When clogging occurs in large cluster size, clogging percentage has less effect on tortuosity change since the cluster affect a few regions while the rest of the PNM is remained unaffected where fluid can find new paths toward the outlets. This is also the reason behind the high termination porosity in large cluster clogging. Clogging appears to have a significant impact on the tortuosity change in TF scenario particularly at high clogging percentages.

Ives and Pienvichitr (1965) assumed that the specific surface area, S is proportional to n^P, hereby, they modify the second part of Kozeny-Carman equation: $K/K_0=(n/n_0)^{3-2P}$ This equation can be simplified by replacing 3-2P with η:

$$\frac{K}{K_0} = (\frac{n}{n_0})^{\eta} \tag{5}$$

Power Law (Eq. 5) has been widely used to describe permeability changes in experimental and modeling studies since it is convenient and only requires porosity, and η as a fitting parameter. Considering tortuosity and specific surface area in permeability calculation by Kozeny-Carman method (Eq. 4), and Power Law, permeability of the soil sample was estimated and compared with the simulation results (Figure 5a for Kozeny-carman, and Figure 5b for Power-law estimation). Figure 5a shows limited improvements in permeability estimations considering porosity, tortuosity and specific surface area in DPF and TF (Eq. 4) compare to estimations based on only porosity (Eq. 3). However, for the LPF (large-cluster), the permeability is not estimated accurately. It can be stated that considering tortuosity and specific surface area in Kozeny-Carman equation leads to partial modifications in permeability estimations. However, the variation of tortuosity and specific surface area in various clogging mechanisms are limited compared to changes in porosity, and would not be sufficient to capture the deviations of permeability between different bio-clogging scenarios. This is clear by comparing the deviations between permeability curves estimated by Eq. 4 with the permeability calculations by PNM simulations (Figure 5a).

Figure 5b shows that power-Law equation can be used to accurately estimate the permeability change in bio-treated soil samples. However, it is crucial to select an appropriate fitting parameter (η) for the given clogging scenario. The estimations present better fits in pore-filling scenarios with distributed, small and medium size clusters. In TF scenario, power-law appears to predict permeability in lower clogging percentages (higher n'), but unable to capture the behavior at higher clogging percentages (e.g. lower n' close to the flow termination moment). The termination porosity in TF is estimated as $n'=0.6$ which is significantly lower than $n'=0.8$ from simulations. The fitting parameter, η, indicates the sensitivity of permeability with porosity. This notion can be demonstrated by the values of η for different scenarios. For example, in TF

scenario, which the normalized porosity is in the range of 1.0 to 0.8, the η is 11.0 which is by far the largest among all the investigated scenarios. The second largest η was found in DPF, the termination porosity of this case is about 0.25, and the slope of simulated permeability also indicate that the permeability changes more notably with porosity change compare to other pore-filling scenarios. Aharonov et al. (1998), and Colon et al. (2004) suggest that any Power Law with exponents lower than 2 is not realistic, which makes the found exponents in this study in an acceptable range.

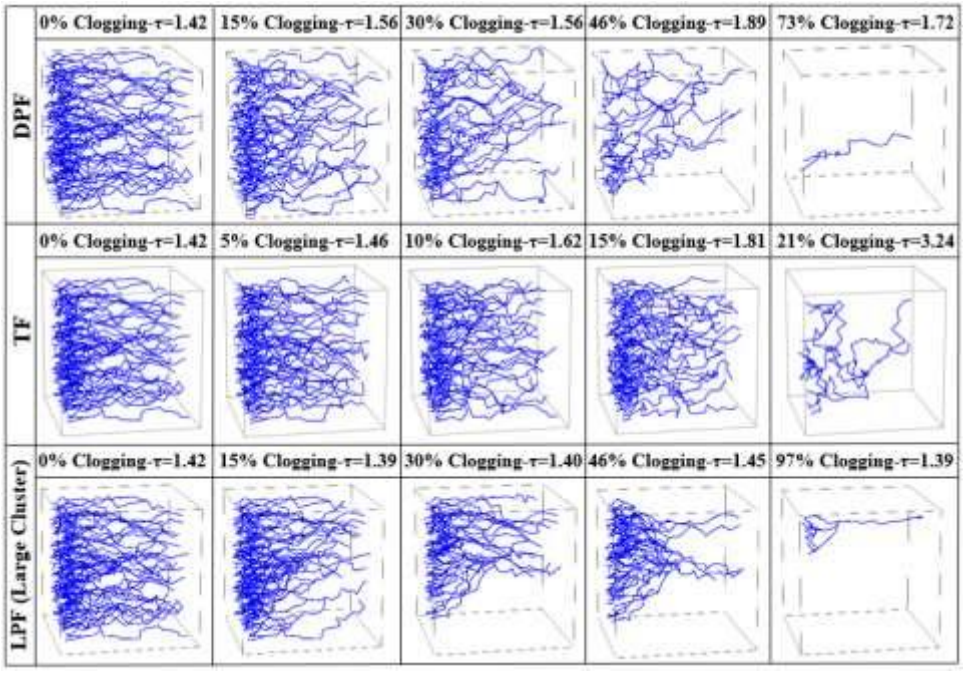

Figure 4. Percolation paths (flow from left to right boundary) in distributed pore-filing, throat-filling, and large cluster clogged PNM with associated tortuosity . The last column presents the percolation path close to termination porosity.

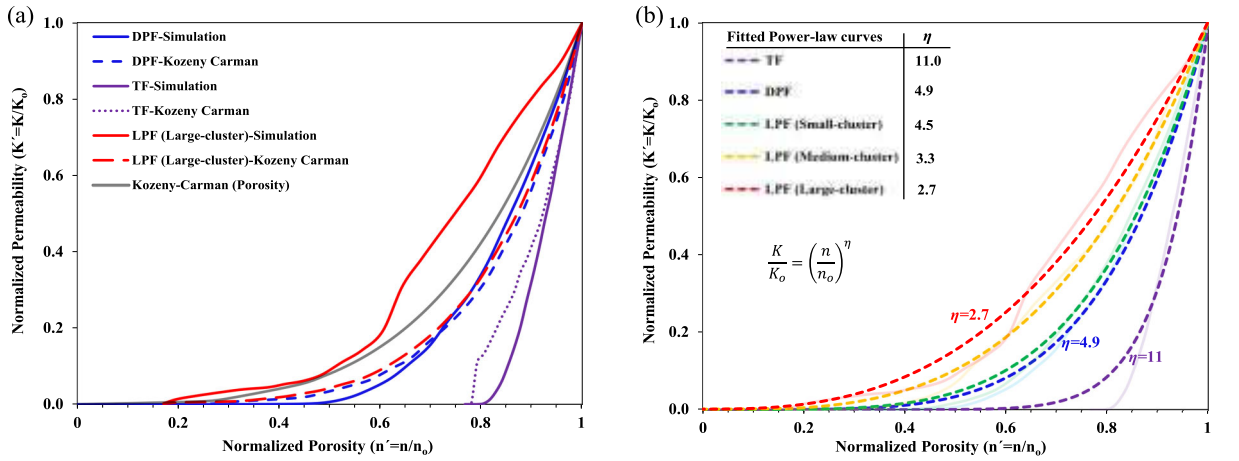

Figure 5. Comparing simulated permeability-porosity relationship with a) modified Kozeny-Carman method (Eq. 4) and b) Power Law method

CONCLUSION

Biological processes involved in bio-mediated soil improvement techniques alters pore-scale characteristics of the soil including pore structure and morphology. In this study, a Pore Network Model (PNM) was extracted from a soil sample to simulate permeability of the sample. Various scenarios of porosity reduction due to biogeochemical activities were simulated. At a given clogging percentage, there is a significant deviation between different clogging scenarios. This finding indicates that the permeability in bio-treated soils is highly hinged to the pore-scale behavior of the bio-products and not only to porosity reduction. Simple Kozeny-Carman relation which solely considers porosity fails to estimate the permeability. Involving all the three terms of porosity, tortuosity and specific surface area into the Kozeny-Carman relation shows partial improvements in the estimations. However, only the porosity can be measured relatively easily in practice. The estimation of permeability via Power Law relations shows high agreements with the numerical results. But the fitting parameter η does not depict any physical meaning to the porous media. In conclusion, inaccuracy and uncertainties involved in the estimation of permeability via analytical/empirical equations such as Kozeny-Carman and Power Law equations suggest that direct numerical simulations, particularly those which are able to capture pore-scale phenomena can play a critical role in studying the impact of bio-geochemical processes on the reactive transport phenomena within the treatment zones.

REFERENCES

Aharonov, E., Tenthorey, E., and Scholz, C. H. (1998). "Precipitation Sealing and Diagenesis: 2. Theoretical Analysis." *Journal of Geophysical Research*. Vol. 103, Issue B10: 969-992.

Colon, C. F., Oelkers, E. H., and Schott, J. (2004). "Experimental investigation of the effect of dissolution on sandstone permeability, porosity, and reactive surface area." *Geochimica et Cosmochimica Acta*, Vol. 68, Issue 4: 805-817.

Cunningham, A. B., Sharp, R. R., Hiebert, R., and James, G. (2003). "Subsurface biofilm barriers for the containment and remediation of contaminated groundwater." *Bioremediation Journal*, Vol. 7, Issue 3-4: 151-164.

DeJong, J. T., Martinez, B. C., Mortensen, B. M., Nelson, D. C., Waller, J. T., Weil, M. H., Ginn, T. R., Weathers, T., Barkouki, T., Fujita, Y., Redden, G., Hunt, C., Major, D., and Tanyu, B. (2009). "Upscaling of bio-mediated soil improvement." *Proc. 17th Int. Conf. Soil Mech. Geotech. Engng.*, Alexandria, 2300-2303.

Dong, H., and Blunt, M. J. (2009). "Pore-Network extraction from micro-computerized-tomography images." *Journal of Phys. Rev. E*. Vol. 80, Issue 3: 06307.

Enouy, R., Li, M., Ioannidis, M. A., and Unger, A. J. A. (2011). "Gas exsolution and flow during supersaturated water injection in porous media: II. Column experiments and continuum modeling." *Advances in Water Resources*, Vol. 34, 15–25.

Hommel, J., Coltman, E., and Class, H. (2018)." Porosity-Permeability relations for evolving pore space: a review with a focus on (bio-)geochemically altered porous media." *Transp Porous Med.* Vol. 124, 589-629.

Ives, K. J., and Pienvichitr, V. (1965). "Kinetics of the filtration of dilute suspensions." *Chemical engineering Science*. Vol. 20, Issue 11: 965-973.

Le Gallo, Y., Bildstein, O., and Brosse, E. (1998). "Coupled Reaction-Flow Modeling of Diagenetic Changes in Reservoir Permeability, Porosity and Mineral Compositions." *Journal of Hydrology* Vol. 209, Issue (1–4): 366–88.

Mahabadi, N., and Jang, J. (2014). “Relative Water and Gas Permeability for Gas Production from Hydrate-Bearing Sediments.” *Geochemistry, Geophysics, Geosystems* Vol. 15, Issue 6: 2346–53.

Mahabadi, N., Dai, S., Seol, Y., Yun, T. S., and Jang, J. (2016). “The Water Retention Curve and Relative Permeability for Gas Production from Hydrate-Bearing Sediments: Pore-Network Model Simulation.” *Geochemistry, Geophysics, Geosystems*. Vol.17, Issue 8: 3099–3110.

Mahabadi, N., and van Paassen, L. A. (2020). “Pore Scale Study of Gas Bubble Nucleation and Migration in Porous Media.” ArXiv Preprint ArXiv:2006.06851, June 11. http://arxiv.org/abs/2006.06851.

McCray, J. E., and Falta, J. W. (1997). “Numerical Simulation of Air Sparging for Remediation of NAPL Contamination.” *Ground Water* Vol. 35, Issue 1: 99–110.

Mostaghimi, P., Blunt, M. J., and Bijeljic, B. (2012). “Computations of absolute permeability on micro-CT images.” *Math Geosci*,Vol. 45: 103-125.

Stallings Young, E. G., Mahabadi, N., Zapata, C. E., and van Paassen, L. A. (2021). “Microbial-induced desaturation in stratified soil conditions.” *Int. J. of Geosynth and Ground Eng*, Vol. 7, Issue, 37.

van Paassen, L. A. (2009). “Microbes Turning Sand into Sandstone, Using Waste as Cement.” In *4th International Young Geotechnical Engineer’s Conference*. Alexandria, Egypt: ISSMGE: 135-138.

Whiffin, V. S., van Paassen, V. A., and Harkes, M. P. (2007). “Microbial Carbonate Precipitation as a Soil Improvement Technique.” *Geomicrobiology Journal* 24 (5): 417–23.